Dynamical Determination of the Innermost Stable Circular Orbit of Binary Neutron Stars

Pedro Marronetti, Matthew D. Duez, and Stuart L. Shapiro*
Department of Physics, University of Illinois at Urbana-Champaign, Urbana, Illinois 61801, USA

Thomas W. Baumgarte†
Department of Physics and Astronomy, Bowdoin College, Brunswick, Maine 04011, USA
(Received 26 September 2003; published 8 April 2004)

We determine the innermost stable circular orbit (ISCO) of binary neutron stars (BNSs) by performing dynamical simulations in full general relativity. Evolving quasiequilibrium (QE) binaries that begin at different separations, we bracket the location of the ISCO by distinguishing stable circular orbits from unstable plunges. We study $\Gamma = 2$ polytropes of varying compactions in both corotational and irrotational equal-mass binaries. For corotational binaries, we find an ISCO orbital angular frequency somewhat smaller than that determined by applying turning-point methods to QE initial data. For the irrotational binaries, the initial data sequences terminate before reaching a turning point, but we find that the ISCO frequency is reached prior to the termination point. Our findings suggest that the ISCO frequency varies with compaction but does not depend strongly on the stellar spin.

DOI: 10.1103/PhysRevLett.92.141101 PACS numbers: 04.30.Db, 04.25.Dm, 97.80.Fk

The emission of gravitational radiation drives the slow inspiral of neutron star and black hole binaries towards their coalescence and merger. Fully general-relativistic numerical simulations are required for the accurate description of the late inspiral and plunge epochs of the binary evolution (see, e.g., [1] for a recent review). While complete orbits of binary black holes have not been numerically simulated yet, simulations of binary neutron star (BNS) mergers are now becoming sufficiently mature to provide results of astrophysical interest (e.g., [2]).

One piece of information of great astrophysical interest is the location of the innermost stable circular orbit (ISCO). The evolution of a binary system occurs in three distinct phases [3]: (1) a slow, adiabatic inspiral phase that is driven by gravitational radiation reaction forces and can be approximated as a sequence of quasicircular orbits; (2) a brief transition phase, where the inward radial motion increases and the orbital motion changes from slow inspiral to rapid plunge; (3) a plunge phase, terminating in the merger of the objects. The ISCO resides within the transition region; its identification is complicated by the fact that it is not arbitrarily sharp and cannot be localized precisely. The gravitational wave quasiperiodic "chirp" signal of the slow binary inspiral ends at about the twice the orbital angular frequency of the ISCO, where it changes its form to a wave signal characteristic of a burst (compare [4]).

Within the framework of Newtonian and post-Newtonian gravity, the ISCO has been determined by different methods (see, e.g., the reviews [5,6] and references therein). Much less is known for fully relativistic binaries. For *corotational* binaries, a turning point on a curve of the binding energy vs separation for quasiequilibrium (QE) models along a sequence of constant rest mass marks the onset of *secular* instability [7,8]. In the following, we will refer to this point as the QE-ISCO. No such theorem exists for *irrotational* binaries or for the onset of *dynamical* instability [9]. Locating the ISCO dynamical instability therefore requires dynamical evolution simulations of the full set of Einstein's equations for the gravitational field, coupled to relativistic hydrodynamics in the case of BNSs.

In this Letter, we present the first attempt to dynamically locate this ISCO. We identify BNS configurations that correspond to stable and unstable circular orbits by evolving binary initial data sets for different separations. The objective is to bracket the location of the ISCO by distinguishing configurations that can maintain quasicircular motion for more than one orbital period and systems that plunge and coalesce in a fraction of that time.

We adopt the QE initial data presented by Marronetti and Shapiro [10], describing two identical neutron stars in quasicircular orbit. These data have been constructed using the conformal thin-sandwich (CTS) decomposition of the constraint equations, together with maximal slicing and spatial conformal flatness. The formalism introduced in [10] allows for a free specification of the spin of the stars in an approximate fashion. In this Letter, we consider corotational binaries as well as "irrotational" binaries [11] with zero (equatorial) fluid circulation, which are believed to be more realistic astrophysically [12]. Sequences of corotating binaries feature a minimum in the binding energy at the QE-ISCO. Irrotational binaries, however, typically terminate before reaching this minimum (see Figs. 7 and 8 in [10]; also [13,14] as well as [1] for more references).

We adopt a $\Gamma = 2$ polytropic equation of state (EOS) for which the maximum rest mass (gravitational mass) of

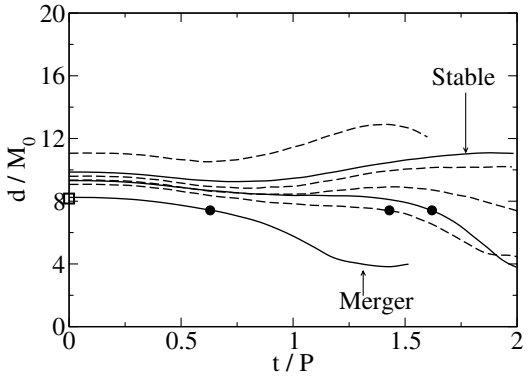

FIG. 1. Coordinate separation vs time for sequences *A*. The separation d is the coordinate distance between points of maximum rest mass density and is given in units of the total rest mass of the binary M_0. The curves show runs with different grid sizes and resolutions which are detailed in Table I. The filled circles mark the time of surface contact for the merger orbits. The empty square on the y axis marks the QE estimation of the ISCO separation.

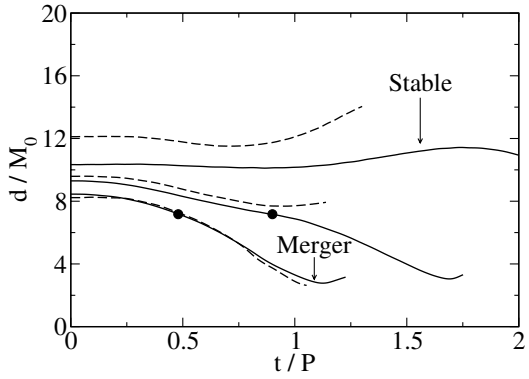

FIG. 2. Coordinate separation vs time for sequences *B*.

a star in isolation in nondimensional units [15] is $m_0 = 0.180$ ($m = 0.164$) with a compaction ratio of $(m/R)_\infty = 0.216$. We study models that have two different compaction ratios in isolation: a moderate value $(m/R)_\infty = 0.142$ (both corotational and irrotational binaries; cases A and B) and a high value $(m/R)_\infty = 0.195$ (only irrotational binaries; case C). These compaction ratios correspond to individual stars with rest masses $m_0 = 0.1469$ and $m_0 = 0.1767$, respectively. The fully general relativistic hydrodynamical code employed for this study has been introduced in Duez *et al.* [16]. We evolve the gravitational fields using the Baumgarte-Shapiro-Shibata-Nakamura formalism [17] with a Courant factor of 0.46. We approximate maximal slicing with a "K driver" and use a "Gamma-driver" shift condition that keeps $\bar{\Gamma}^i \equiv \bar{\gamma}^{lm}\bar{\Gamma}^i_{lm}$ approximately constant. The simulations were performed on uniform Cartesian grids in a reference frame that rotates with the binary, which improves conservation of angular momentum [16,18] and reduces the spurious eccentricities of the stable orbits. In all cases presented here, the spatial volume covered by the grids is completely enclosed by the light cylinder (defined by coordinate radius $R_L = 1/\Omega_{\rm orb}$). A more detailed description of the evolution of the gravitational and hydrodynamical fields, the boundary conditions, and their numerical implementation can be found in Duez *et al.* [16].

Figures 1–3 show the evolution of the coordinate separation d between maximum baryonic density points in each star for cases A, B, and C [19]. The filled circles mark the points of surface contact for those runs that result in a merger. In each plot, we present results for different grid resolutions and bounding box sizes, which are listed in Table I. We use the highest quality results to bracket the ISCO; these are labeled as *Stable* and *Merger* in the plots. Results obtained on smaller computational grids agree with these brackets fairly well. Note that all three merger cases experience surface contact (and the related mass interchange) well after the start of the inspiral plunge. The ISCO parameters for each of the three cases are estimated as the average of the parameters corresponding to the bracketing orbits labeled *Stable* and *Merger* on each figure, while the "errors" span the difference. We note that these "errors" are partly due to numerical errors (see below), and partly by the conceptional difficulty of defining a sharp "ISCO." The results are included in Table II. For the corotating sequence A, we also compare with the QE-ISCO at the QE turning point. The irrotational sequences considered in this paper terminate before reaching a turning point (compare [13,14]). The termination of a sequence indicates that equilibrium models do not exist at smaller separations, but since the numerical determination of this point relies on the breakdown of a numerical (equilibrium) code, its accuracy is somewhat uncertain. For both sequences, we find that the ISCO is reached before the sequence terminates. For the irrotational sequence C, one can also compare with the first-order post-Newtonian ellipsoidal results of

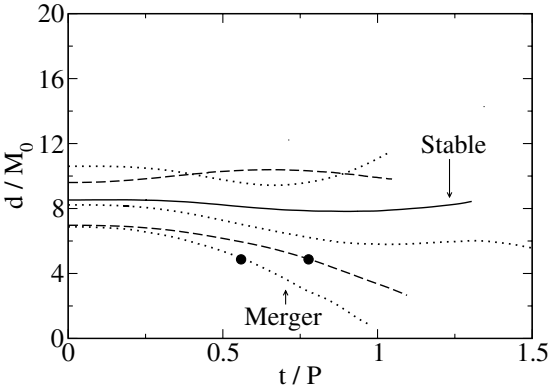

FIG. 3. Coordinate separation vs time for sequences *C*.

TABLE I. Grid sizes and resolutions. The resolution (Res.) is given in number of grid points across the stellar diameter. The bounding box length B gives the extent of the physical space covered in each direction in units of total rest mass M_0 (i.e., the numerical grid spans from$[-B, 0.0, 0.0]$ to $[B, B, B]$ since we make use of the equatorial and π symmetries of the systems).

Case	Figure	Curves	Res.	B/M_0	Grid points	Res.	Box
A	1	Dashed	20	18.7	$64^2 \times 128$	Low	Large
A	1	Solid	40	18.7	$128^2 \times 256$	High	Large
B	2	Dashed	20	18.7	$64^2 \times 128$	Low	Large
B	2	Solid	40	18.7	$128^2 \times 256$	High	Large
C	3	Dotted	30	15.2	$128^2 \times 256$	Low	Large
C	3	Dashed	40	11.5	$128^2 \times 256$	High	Small
C	3	Solid	40	15.5	$172^2 \times 344$	High	Large

Lombardi *et al.* [20], who find an angular velocity of $\Omega m_0 = 0.0226$ for $(m/R)_\infty = 0.2$ binaries.

We consistently find that orbits become unstable before the onset of instability as determined by QE methods, meaning at a smaller orbital frequency. This is not surprising, since the orbital decay becomes fairly rapid just outside the QE-ISCO (compare, e.g., Fig. 2 in [4]), so that our criterion for merger orbits applies to those binaries. This result is also consistent with earlier suggestions that the transition through the ISCO may be fairly gradual [3]. The similarity between the corotating and irrotational values for the $(m/R)_\infty = 0.142$ orbits suggests that the dependence of the ISCO parameters on the stellar spins is not strong.

During all simulations, we monitored the Hamiltonian and momentum constraints as well as the conservation of the total Arnowitt-Deser-Misner (ADM) mass M and angular momentum J [21] (the rest mass M_0 is conserved identically in our evolution scheme). An example of these for case B is shown in Fig. 4. In all our simulations, all quantities are conserved very well up to merger, after which hydrodynamical effects including shocks and shear are handled only crudely by our artificial viscosity scheme. Stable runs ultimately break down due to accumulation of numerical error. We find that the latter is sometimes dominated by hydrodynamical effects, leading to deviations in the angular momentum, and sometimes by gravitational effects, leading to violations of the constraint equations. These effects are improved by increasing the grid resolution and the separation to the outer boundaries, as well as using a coordinate system that rotates with the binary as closely as possible.

We present prototype simulations to determine dynamically the ISCO of BNSs. Evolving QE initial data at different separations, we bracket the ISCO by distinguishing stable orbits, which remain in approximately circular orbit for well over a period, from unstable ones, which decay within a period. The uncertainty in our results is caused both by numerical error and the conceptual difficulty in defining a sharp ISCO.

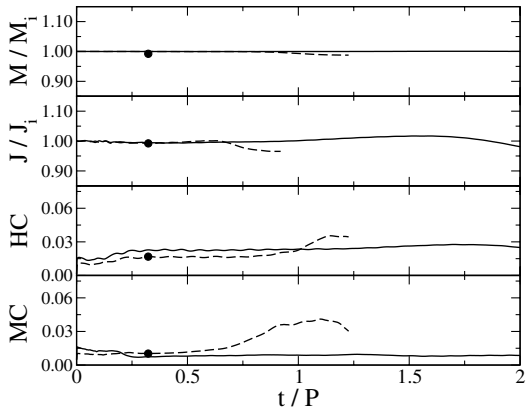

FIG. 4. Quality control for the $(m/R)_\infty = 0.142$ irrotational runs. We show from top to bottom the total gravitational mass, angular momentum, the Hamiltonian constraint, and the average of the components of the momentum constraint vs time [22]. The curves correspond to the runs from Fig. 2 labeled as *Stable* (solid lines) and *Merger* (dashed lines). The filled circle marks the time of surface contact for the merger orbit.

Consistent with earlier results [3,4], we find that binary orbits start to plunge somewhat outside of the "QE-ISCO" as determined by turning-point methods applied to QE initial data, resulting in a cutoff in gravitational "chirp" signals at somewhat smaller frequency. Our preliminary results also seem to indicate that the dependence of the ISCO parameters on the stellar spins is not very strong.

One source of error is our assumption of zero radial velocity in our binary initial data. More realistic initial data at finite binary separation would incorporate a radial velocity that corresponds to the nonzero rate of inspiral at that separation. Miller [23] indicates that this approximation may lead to non-negligible error, especially for black hole binaries. However, for the neutron star binaries and separations we consider here, the radial velocities would be at most 1%–3% of the tangential velocity [4,23]. Consequently, the error introduced by neglecting this component is likely to be smaller than the error bars already provided in Table II.

It was recently pointed out that, in dynamical evolutions of CTS initial data describing corotating BNSs, the four-velocity u^α quickly deviates from being proportional to an exact helicoidal Killing vector, as assumed in constructing the initial models [24]. We confirm this result but find that this deviation arises from a small readjustment of the gravitational fields [25], and not from appreciable changes in the density and velocity profiles. We find no evidence of a significant breakdown of quasiequilibrium for stable orbits, and any spurious orbital eccentricities sharply decrease with increasing grid size.

It is a pleasure to thank Hwei-Jang Yo for useful discussions. Most of the calculations were performed at the National Center for Supercomputing Applications at the University of Illinois at Urbana-Champaign (UIUC). This

TABLE II. Summary of our binary cases A, B, and C and results for their ISCO. For each sequence, we show the rotation state, the rest mass of the individual stars m_0, the compaction in isolation $(m/R)_\infty$, the total initial ADM mass M_i and angular momentum J_i/M_i^2, as well as the binary coordinate separation at the ISCO d/M_0 (where M_0 is the total rest mass $2m_0$) and the corresponding orbital angular velocity Ωm_0. For the corotational sequence, we also compare with the QE result for Ωm_0 [10]. The wave frequency at the ISCO is $f_{\rm GW}$ and $m_{1.4}$ is the stellar gravitational mass in units of $1.4M_\odot$.

Case	Rotation	m_0	$(m/R)_\infty$	M_i	J_i/M_i^2	d/M_0	Ωm_0	Ωm_0 (QE)	$f_{\rm GW} m_{1.4}$ (kHz)
A	Corotating	0.1469	0.142	0.2708 ± 0.0001	1.08 ± 0.01	9.0 ± 0.8	0.0162 ± 0.0021	0.0179	0.697
B	Irrotational	0.1469	0.142	0.2702 ± 0.0003	0.97 ± 0.04	9.4 ± 0.9	0.0154 ± 0.0022	⋯	0.662
C	Irrotational	0.1767	0.195	0.3171 ± 0.0009	0.93 ± 0.04	7.7 ± 0.8	0.0199 ± 0.0029	⋯	0.838

paper was supported in part by NSF Grants No. PHY-0090310 and No. PHY-0205155, NASA Grant No. NAG 5-10781 at UIUC, and NSF Grant No. PHY-0139907 at Bowdoin College. P. M. gratefully acknowledges financial support through the Fortner Fellowship at the University of Illinois at Urbana-Champaign (UIUC).

*Department of Astronomy & NCSA, University of Illinois at Urbana-Champaign, Urbana, IL 61801, USA
†Department of Physics, University of Illinois at Urbana-Champaign, Urbana, IL 61801, USA.

[1] T.W. Baumgarte and S. L. Shapiro, Phys. Rep. **376**, 41 (2003).
[2] M. Shibata and K. Uryū, Phys. Rev. D **61**, 064001 (2000); M. Shibata and K. Uryū, Prog. Theor. Phys. **107**, 265 (2002).
[3] A. Ori and K. S. Thorne, Phys. Rev. D **62**, 124022 (2000); A. Buonanno and T. Damour, Phys. Rev. D **62**, 064015 (2000).
[4] M. D. Duez, T.W. Baumgarte, S. L. Shapiro, M. Shibata, and K. Uryū, Phys. Rev. D **65**, 024016 (2001).
[5] T.W. Baumgarte, in *Astrophysical Sources of Gravitational Radiation*, edited by J. M. Centrella (AIP, New York, 2001).
[6] F. A. Rasio and S. L. Shapiro, Classical Quantum Gravity **16**, R1 (1999).
[7] J. L. Friedman, J. R. Ipser, and R. D. Sorkin, Astrophys. J. **325**, 722 (1988).
[8] T.W. Baumgarte, G. B. Cook, M. A. Scheel, S. L. Shapiro, and S. A. Teukolsky, Phys. Rev. D **57**, 6181 (1998).
[9] Approximating the stars as ellipsoids, it has been shown that the dynamical orbital instability occurs quite close to the secular instability for irrotational binaries in both Newtonian and first-order post-Newtonian theory [D. Lai, F. A. Rasio, and S. L. Shapiro, Astrophys. J. Suppl. **88**, 205 (1993)].
[10] P. Marronetti and S. L. Shapiro, Phys. Rev. D **68**, 104024 (2003).
[11] For simplicity, in the reminder of the paper we will refer to the zero circulation models as irrotational. See [10] for comparisons between these models and irrotational binaries.
[12] C. S. Kochanek, Astrophys. J. **398**, 234 (1992); L. Bildsten and C. Cutler, Astrophys. J. **400**, 175 (1992).
[13] K. Uryū, M. Shibata, and Y. Eriguchi, Phys. Rev. D **62**, 104015 (2000).
[14] E. Gourgoulhon, P. Grandclément, K. Taniguchi, J.-A. Marck, and S. Bonazzola, Phys. Rev. D **63**, 064029 (2001).
[15] We set $G = c = \kappa = 1$, where κ is the polytropic constant of the EOS: $P = \kappa\rho_0^\Gamma$. For scaling with κ, see Ref. [8].
[16] M. D. Duez, P. Marronetti, S. L. Shapiro, and T.W. Baumgarte, Phys. Rev. D **67**, 024004 (2003).
[17] M. Shibata and T. Nakamura, Phys. Rev. D **52**, 5428 (1995); T.W. Baumgarte and S. L. Shapiro, Phys. Rev. D **59**, 024007 (1999).
[18] F. D. Swesty, E. Y. Wang, and A. C. Calder, Astrophys. J. **541**, 937 (2000).
[19] The time coordinate has been transformed into fractions of the initial orbital period. Note that the periods differ for binaries at different separation.
[20] J. C. Lombardi, F. A. Rasio, and S. L. Shapiro, Phys. Rev. D **56**, 3416 (1997).
[21] The total angular momentum like the gravitational mass is not strictly conserved due to the emission of gravitational waves. However, the loss rate of angular momentum for a typical orbit at these separations is of the order of 1% to 2%. Deviations exceeding these values therefore indicate numerical error.
[22] This figure presents the L_2 norm of the constraint residuals. The details of these plots as well as the normalizations used here can be found in [16]. In this Letter, the momentum constraint curve shows the average of the three spatial components.
[23] M. Miller, gr-qc/0305024.
[24] M. Miller and W. M. Suen, gr-qc/0301112; M. Miller, P. Gressman, and W. M. Suen, gr-qc/0312030.
[25] Small amounts of spurious radiation present in the initial data are radiated away, leaving M and J nearly unchanged.